



Synthesis and characterization of water-soluble free-base, zinc and copper porphyrin–oligonucleotide conjugates

Angela Mammana^a, Tomohiro Asakawa^a, Klaus Bitsch-Jensen^a, Amanda Wolfe^a, Saireudee Chaturantabut^a, Yuko Otani^a, Xiaoxu Li^b, Zengmin Li^b, Koji Nakanishi^a, Milan Balaz^{a,*}, George A. Ellestad^{a,*}, Nina Berova^{a,*}

^a Department of Chemistry, Columbia University, 3000 Broadway, New York, NY 10027, USA

^b Columbia Genome Center and Department of Chemical Engineering, Columbia University, 1150 St. Nicholas Avenue, New York, NY 10032, USA

ARTICLE INFO

Article history:

Received 18 April 2008

Revised 7 May 2008

Accepted 9 May 2008

Available online 15 May 2008

Keywords:

Porphyrin

DNA

Oligonucleotide

Metallation

Phosphoramidite

MALDI-TOF

ABSTRACT

We describe the synthesis and characterization of a series of water-soluble free-base, zinc, and copper porphyrin–oligonucleotide (ODN) conjugates. A non-charged tetraarylporphyrin was directly attached to the 5'-position of thymine via a short amide linker. Such a linker should allow for rigid connection to the adjacent nucleobases, thus increasing the sensitivity for monitoring conformational changes of the ODNs by electronic circular dichroism due to capping effects or ligand binding. Two complementary synthetic approaches have been used to incorporate porphyrin chromophores into the DNA. In the first approach a porphyrin carboxylic acid is conjugated to 5'-amino-ODN. In the second approach the phosphoramidite of the porphyrin-amido-thymidine is coupled to 5'-hydroxy-ODN using standard automated phosphoramidite chemistry. In both cases a spontaneous metallation of the free-base porphyrin in porphyrin–DNA conjugates was observed during the porphyrin–DNA conjugate cleavage from the solid support and its consequent deprotection using concentrated aqueous ammonia. Zinc and copper porphyrin–DNA conjugates were isolated by HPLC and characterized together with the anticipated free-base porphyrin–DNA conjugate. Authentic zinc and copper porphyrin–DNA conjugates were intentionally prepared from intentionally metallated porphyrins to compare their spectroscopic and HPLC characteristics with isolated metallospecies and to confirm the spontaneous metallation.

© 2008 Elsevier Ltd. All rights reserved.

1. Introduction

The 'bottom-up' approach to produce functional, self-organizing nanodevices from molecular building blocks giving a precise arrangement of atoms and molecules in three dimensions is most likely to meet the needs of future technologies. Chromophore arrays often exhibit different spectroscopic properties from monomers that they are assembled from. Porphyrin assemblies have been extensively investigated for their promising photonic properties. Many nature-inspired porphyrin assemblies have been developed aiming for efficient light collection and energy transfer.^{1–6}

DNA has become very attractive as a molecular scaffold for precise positioning of desired molecules on the nanoscale due to its molecular recognition and mechanical properties.^{7–9} Stacking interactions between nucleobases are, in addition to hydrogen-bonding, the key factors that stabilize the double-stranded DNA helix and determine DNA's secondary and tertiary structure.^{10,11}

* Corresponding authors. Present address: Oxford University, Department of Chemistry, Mansfield Road, Oxford OX1 3TA, UK (M.B.). Tel.: +1 212 854 3934; fax: +1 212 932 1289.

E-mail addresses: mb2402@columbia.edu (M. Balaz), gae2104@columbia.edu (G.A. Ellestad), ndb1@columbia.edu (N. Berova).

Exposed DNA termini base pairs represent the weakest link in base-pairing fidelity and potential problems in the self-assembly process. A well-defined arrangement of chromophores is an important tool for novel applications in material sciences and nanotechnology. In order to increase the base pair fidelity at the DNA termini, several synthetic strategies have been introduced. The capping of the oligonucleotides termini with small molecules is a useful method to improve the properties of their natural counterparts such as nucleobase pairing fidelity,^{12,13} duplex stability,^{14–17} or resistance against exonuclease degradation.¹⁸ Capping is usually favored by covalently attaching small molecules to the 3' or 5' DNA termini.

Porphyrins are one of the most studied DNA binding agents, and there are many reports on porphyrin–DNA interactions.^{19–23} However, most studies focused on interactions between free (non-covalently attached) cationic porphyrins and polymeric DNA. Although the first porphyrin–oligonucleotide conjugates were synthesized 15 years ago,^{24,25} there are only few recent studies focusing on the structural and spectroscopic properties of these conjugates,^{26–28} on interactions between porphyrins,^{29–31} and on interactions between porphyrin and DNA^{32,33} in porphyrin–DNA conjugates. We were the first to study the through space exciton coupling between two porphyrins covalently attached to

a short DNA sequence (DNA as the helical scaffold), and the effect of covalently attached porphyrins on DNA structure and stability. We had reported previously that porphyrins linked to one of the DNA termini can communicate through space upon formation of double-stranded DNA resulting in an exciton-coupled circular dichroic signal.²⁹ This signal is very diagnostic and can serve as internal probes for DNA conformational changes.^{29,34} Recently we have shown that a porphyrin, covalently attached to the 5' end of a short non-self-complementary oligonucleotide, can stabilize the non-Watson–Crick base pairing between guanine and adenine and promote the formation of the right-handed A-like double-stranded DNA via termini capping.¹⁷ Additionally, porphyrin chromophores also served as a sensitive internal circular dichroic sensor of the newly formed secondary structure.¹⁷ Better understanding of porphyrin–DNA interactions will help us to rationally design new materials and predict their photophysical and photochemical properties.

The position, length, and type of the linker between porphyrin and DNA play an important role in the porphyrin/DNA interfacial interaction and strongly dictate/influence the interactions between the porphyrin and neighboring nucleobases. We anticipate that a short and non-charged linker will promote a close non-covalent stacking interaction between porphyrin and exposed DNA termini.

In this paper we present the synthesis of water-soluble 5'-porphyrin–DNA conjugates and 5'-metalloporphyrin–DNA conjugates with a short 5'-amide linker between porphyrin chromophore and the nucleobase. We have rationalized the origin of the unexpected spontaneous metallation and discuss the different spectroscopic and HPLC properties of the metalloporphyrin–DNA conjugates.

2. Results and discussion

2.1. Synthesis of porphyrin–DNA conjugates

Porphyrins were attached to the 5' position of self-complementary oligonucleotide sequences via a short, rigid amide linkage. Annealing of the self-complementary porphyrin modified ODN will provide a DNA duplex having one porphyrin cap at each end. The amide bond was chosen because such a linkage would provide a shorter and less flexible connection to the adjacent nucleobases, thus increasing the sensitivity for monitoring con-

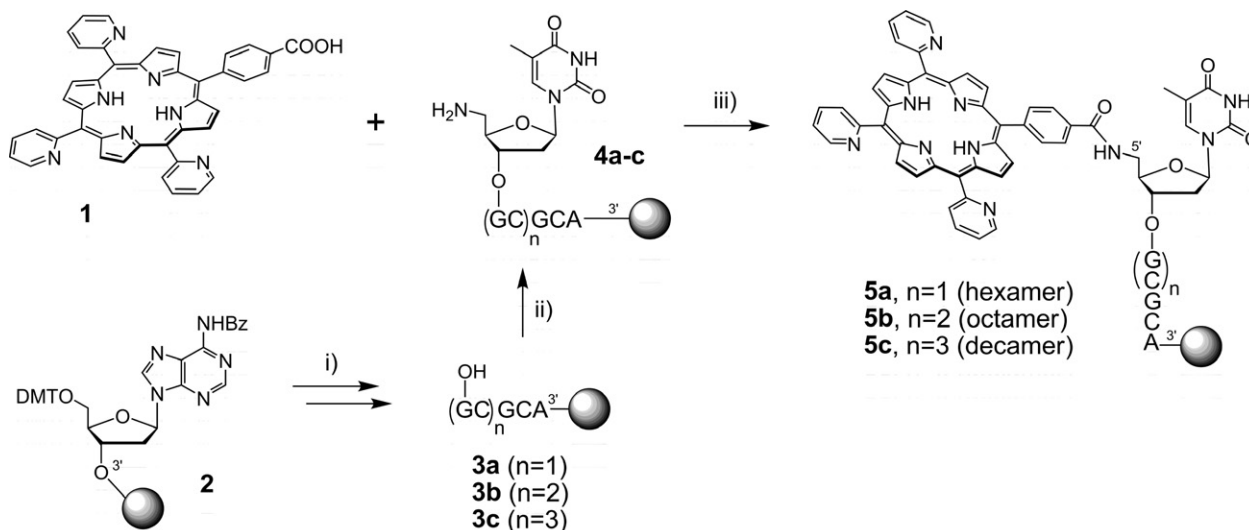
formational changes of the DNAs via long-range exciton-coupled CD. Such a linker also provides good control over the position of the porphyrin on the DNA and prevents unwanted porphyrin intercalation. The short DNA sequence 5'-TGCGCGCA was selected for our study. We used two different strategies for the synthesis of the 5'-amido linked tetraarylporphyrin oligonucleotide. In the first approach porphyrin carboxylate **1** is conjugated to solid supported 5'-amino-ODNs **4a–c** (**4a**: hexamer, **4b**: octamer, **4c**: decamer) using benzotriazol-1-yl-oxytriethylphosphonium hexafluorophosphate (PyBOP) and diisopropylethylamine (DIPEA, Scheme 1). In the second approach the 5'-porphyrin-amido-thymidine 3'-phosphoramidite **9** is synthesized and then coupled to 5'-hydroxy-ODNs **10a–c** under standard phosphorylation conditions (Scheme 3).

2.1.1. Approach 1

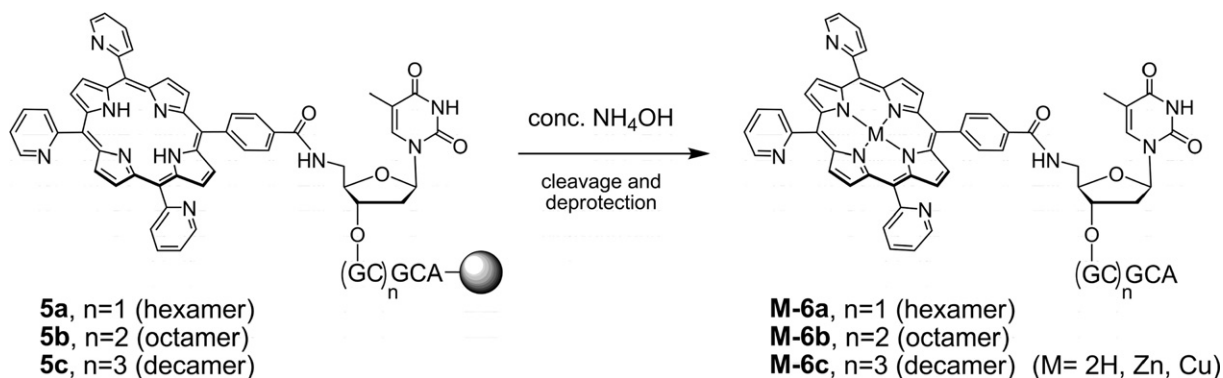
As outlined in Scheme 1, porphyrin carboxylic acid **1** was conjugated manually to the exposed 5'-amino-group of thymidine in ODNs **4a–c**. ODNs **4a–c** were prepared from unmodified ODNs 5'-hydroxy-(GC)_nGCA-support **3a–c** ($n = 1–3$) using standard methodologies on a DNA synthesizer. A 1000 Å controlled pore glass (CPG) solid-support cartridge was critical as the CPG cartridge with smaller 500 Å pores was much less successful for the attachment of the bulky porphyrin carboxylic acid **1**. The porphyrin–DNA conjugates **5a–c** were then cleaved from the CPG beads and deprotected with concentrated aqueous ammonia at room temperature overnight (Scheme 2). The aqueous ammonia was removed under vacuum and the crude reaction mixture analyzed by mass spectrometry and reverse phase HPLC (RP-HPLC) to provide **M-6a–c**.

2.1.2. Approach 2

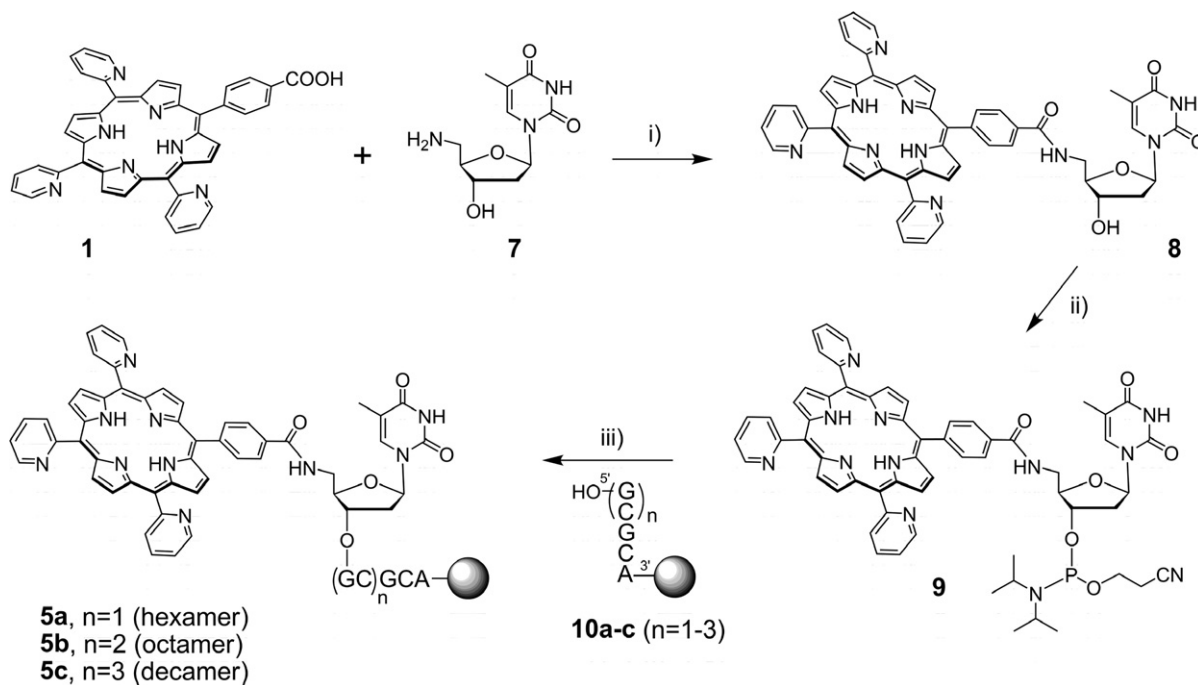
The synthesized 5'-amino-3'-hydroxy thymidine^{35,36} **7** was reacted with the free-base trispyridylphenylporphyrin carboxylate³⁷ **1** (Scheme 3). The resulting 5'-porphyrin-amido-thymidine **8** was converted to phosphoramidite **9**, purified by flash column chromatography, and characterized by ¹H and ³¹P NMR. ³¹P NMR showed two signals resulting from two diastereomers around the pyramidal phosphorous atom formed (Fig. 1). Porphyrin–phosphoramidite **9** was then reacted with solid supported oligonucleotides **10a–c** (**10a**: hexamer, **10b**: octamer, **10c**: decamer) under standard phosphoramidite chemistry. Concentrated aqueous ammonia was used



Scheme 1. Approach 1: synthesis of porphyrin–oligonucleotide conjugates **5a**, **5b**, and **5c**. Reagents: (i) standard automated cyanoethyl-phosphoramidite solid-phase chemistry, DNA synthesizer; (ii) 5'-amino-thymine-phosphoramidite; (iii) PyBOP, DIPEA, DMF, on-column synthesis.



Scheme 2. Cleavage from the solid support and the deprotection of the porphyrin–DNA conjugates **5a**, **5b**, and **5c**.



Scheme 3. Approach 2: synthesis of porphyrin–oligonucleotide conjugates **5a**, **5b**, and **5c**. Reagents: (i) EDC, DCM; (ii) 2-cyanoethyl- N,N -diisopropylchlorophosphoramidite, DIPEA, DCM; (iii) DCM, activation reagent (acetonitrile/tetrazole) then oxidation.

for cleavage of the porphyrin–oligonucleotide conjugates **5a-c** from the solid support and DNA deprotection (Scheme 2). The aqueous ammonia was removed under vacuum and the crude reac-

tion mixture analyzed by mass spectrometry and reverse phase HPLC.

2.2. Analysis of porphyrin–DNA conjugates **6a**, **6b**, and **6c**

2.2.1. MALDI-TOF and HPLC

MALDI-TOF analysis of the crude porphyrin–octamer **6b** indicated the presence of the expected free-base porphyrin–DNA **2H-6b** with a MW of 3051 ± 3 . In addition, a species with a MW of 3114 ± 3 ($3051 + 63$) was observed, which seemed to be a metalloporphyrin–8-mer conjugate containing either copper(II) (+63.5) or zinc(II) (+65.4) in the porphyrin coordination center. The HPLC profile of **6b** also showed two major peaks (Fig. 2). Porphyrin–DNA conjugate **6b** was dissolved in water and injected onto the HPLC with a gradient of buffer (hexafluoroisopropanol and triethylamine) and methanol at a flow rate of 1 mL/min (see Section 4.2.6. for further details).³⁷ The first (more polar) compound eluted at 47.1 min gave the anticipated MW of 3051 ± 3 for free-base porphyrin–ODN **2H-6b**. The second peak eluted at 48.6 min (less

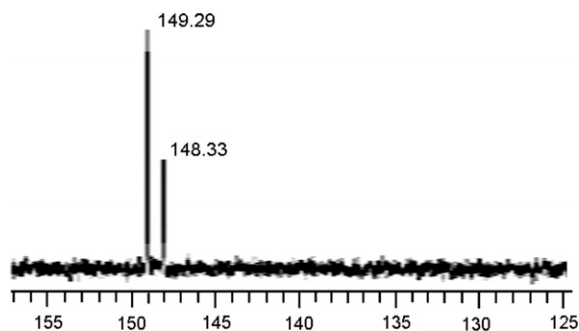


Figure 1. ^{31}P NMR spectrum of 5'-porphyrinthymidine 3'-phosphoramidite **9**.

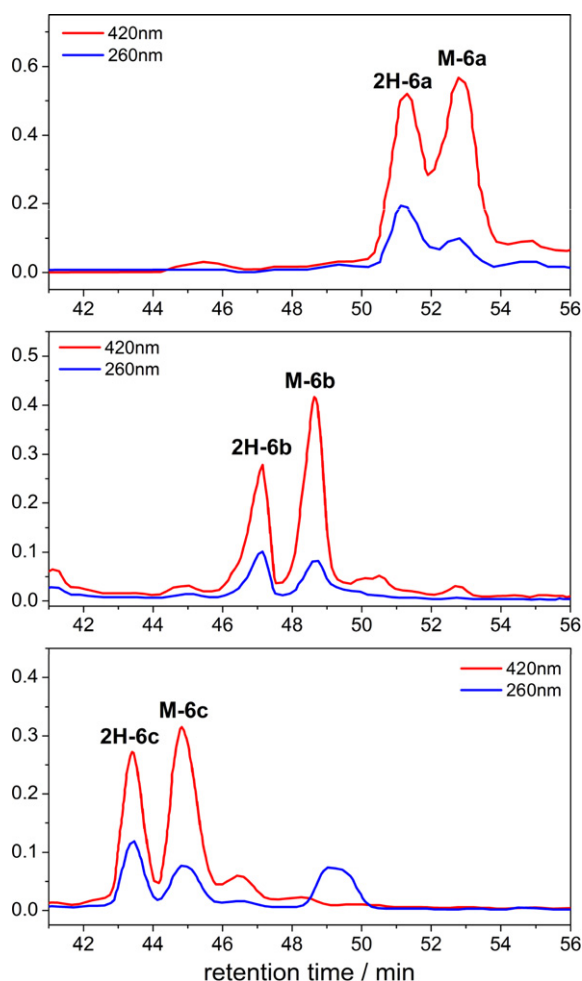


Figure 2. HPLC profiles of crude porphyrin–DNA conjugates **6a** (porphyrin-hexamer, top), **6b** (porphyrin-octamer, middle) and **6c** (porphyrin-decamer, bottom) monitored at two different wavelengths, 260 nm and 420 nm.

polar) gave a MW of 3114 ± 3 . However due to the small mass differences between zinc and copper (difference of two mass units) MALDI-TOF spectrometry was unable to tell with certainty if we had synthesized zinc porphyrin–ODN **Zn-6b** or copper porphyrin–ODN **Cu-6b** (together called **M-6b**). Similar results have been obtained in the synthesis of porphyrin-hexamer **6a** and porphyrin-decamer **6c**. Two major products were always observed, the first one corresponding to the desired free-base porphyrin–DNA conjugates, and the second one to the metalloporphyrin-conjugates **M-6**, sometimes **Zn-6** or **Cu-6**, and sometimes both. MALDI-TOF data, HPLC retention times, and HPLC profiles for porphyrin–DNA conjugates **6a**, **6b**, and **6c** are summarized in Table 1, in Figure 2, and in Figure S1–S6 (see Supplementary material).

Table 1
HPLC and MALDI-TOF-MS data of products formed in the synthesis of porphyrin–DNA conjugates **6a**, **6b**, and **6c**

Porphyrin–DNA	Calculated molecular weight	HPLC retention time ^a (min)	MALDI	MALDI difference ^b
6a (hexamer)	2434.6	51.2	2435.2	+0.6
		52.8	2497.1	+62.5
6b (octamer)	3052.7	47.1	3054.51	+1.81
		48.6	3112.0	+62.1
6c (decamer)	3670.8	43.5	3673.2	+2.4
		44.9	3737.8	+67.0

^a See Table 3 for HPLC elution conditions.

^b Difference between calculated and experimental molecular masses.

2.2.2. UV–vis absorption spectra

Because of the ambiguity of MALDI-TOF data we turned our attention to absorption spectra of the porphyrin–ODNs **6a–c**. It is well known that the UV–vis profile of each porphyrin and metalloporphyrin is very diagnostic.³⁸ UV–vis spectrum of first eluted free-base porphyrin–DNA conjugate **2H-6** showed a Soret absorption band at 422 nm and three Q bands at 516, 554, 585 nm. This spectral profile is typical of the free-base porphyrins. Examination of the UV spectrum of less polar **M-6b** (elution time 48.6 min) enabled us to assign this species to the zinc(II) porphyrin–DNA conjugate **Zn-6b**. The UV–vis spectrum porphyrin region showed a maximum at 425 nm and two smaller Q bands at 558 and 594 nm characteristic of a zinc porphyrins.³⁸ Surprisingly, using different batches of ammonia, a copper porphyrin conjugate, **Cu-6b**, was isolated with a Soret band at 418 nm and only one Q band at 541 nm. Figure 3 shows UV–vis spectra of all three porphyrin–ODNs, free-base conjugate **2H-6b**, zinc conjugate **Zn-6b**, and copper conjugate **Cu-6b**.

The HPLC analysis of porphyrin–DNA conjugates prepared via approach 2 showed one major product with retention time of the metallated porphyrin–DNA conjugate **M-6b**. The MALDI-TOF spectrum showed the molecular weight of 3114 (**2H-6b** + 63). As with the results from Approach 1, we have explained the origin of these unexpected compounds **M-6b** by the incorporation of copper(II) (atomic weight = 63.5 g/mol) or zinc(II) (atomic weight = 65.4 g/mol) into the porphyrin coordination center. The UV–vis spectrum was also used to identify the presence of zinc and copper porphyrin–ODN conjugate **M-6b**.

2.3. Synthesis of metalloporphyrins M-1 and metalloporphyrin–DNA conjugates M-6b

To confirm the origin of the metalloporphyrin–DNA conjugate(s), isolated along with the free-base porphyrin–DNA conjugate, we synthesized the zinc tetrapyrrolylporphyrin carboxylate, **Zn-1**, and the corresponding **Cu-1**. Free-base porphyrin **1** was metallated using zinc acetate or copper acetate, respectively. Porphyrin carboxylate **1** was dissolved in chloroform and 10 equivalents of corresponding acetate was added. The reaction mixture had to be heated to reflux as metallation was not observed at room temperature. The synthesized metalloporphyrins **Zn-1** and **Cu-1** were found to be of sufficient purity to be directly conjugated with 5'-amino-ODN **4b** attached to the solid support using identical conditions as for free-base porphyrin **1**. After cleavage and deprotection with concentrated ammonia, porphyrin modified ODNs **Zn-6b** and **Cu-6b** were purified by RP-HPLC (see Figures S8 and S9, Supplementary material) and analyzed by UV–vis spectroscopy and MALDI-TOF-MS. The UV–vis spectra were identical with those of previously isolated zinc and copper porphyrin conjugates **6b** resulting from metal contamination. Although the free-base conjugate **2H-6b** elutes typically earlier than the metal conjugates (see Fig. 2), we observed negligible or no difference in retention time between copper and zinc conjugates when authentic samples of the last two were co-injected. Table 2 summarizes the UV–vis characteristics of synthesized porphyrin-octamers **M-6b**.

2.4. Spontaneous metallation of porphyrin–DNA conjugates 6a, 6b, and 6c

We believe that the source of the metallation is the concentrated aqueous ammonia used for the cleavage/deprotection of porphyrin–DNA conjugates. It is known that concentrated ammonia contains numerous trace metals and that the long exposure of the matrix during the ODN cleavage and deblocking of the assembled conjugate gives enough time for metallation to take place. That the concentrated ammonia is the source of the metals is fur-

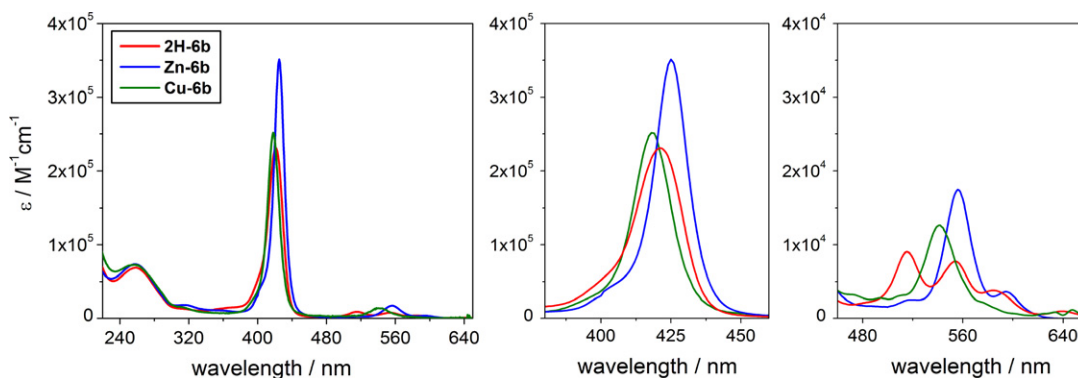


Figure 3. UV-vis absorption spectrum of porphyrin-8-mer conjugates **2H-6b** (red), **Zn-6b** (blue), and **Cu-6b** (green). Soret band region (middle) and Q band region (right) of UV-vis spectra were expanded. Conditions: 50 mM potassium phosphate buffer, pH 7.0.

Table 2

UV-vis absorption characteristics of porphyrin DNAs **2H-6b**, **Zn-6b**, and **Cu-6b** measured in 50 mM K-phosphate buffer, pH 7.0

Porphyrin-octamers	Soret band ^a	Q band
2H-6b	422 nm (230,600)	516, 554, 585 nm
Zn-6b	425 nm (351,038)	557, 594 nm
Cu-6b	418 nm (251,546)	541 nm

^a Absorption wavelength (extinction coefficient).

ther corroborated by the fact that different ratios of the metallated species were obtained depending on the source of the aqueous ammonia (results not shown). The small scale of the synthesis (1 μ M) and overall low yields of the porphyrin–DNA coupling (<10%) undoubtedly contribute to the high level metallation as well. The spontaneous metallation of porphyrin in ODN conjugates **6a**, **6b**, and **6c** points to the need for caution in the use of concentrated ammonia in the deprotection step involving porphyrins.

It should be mentioned, however, that unconjugated free-base porphyrin carboxylate **1** only underwent metallation with an excess of metal acetates (~10 equiv) under reflux (see below). The mild experimental conditions under which we observe metal complexation of the porphyrin conjugates are inconsistent with the conditions necessary for complexation of free porphyrin **1**. Based on the MALDI-TOF-MS of crude porphyrin–ODN conjugate of different preparations, the amount of metalloconjugates present ranged from 10% to 50% of the free-base porphyrin–ODN conjugates. Additional porphyrin metallation takes place during the HPLC purification (50 °C) to give a mixture of unmetallated and metallated porphyrin conjugates in a ratio of ca. 40/60, respectively, based on HPLC product peak areas (see Fig. 2). Thus it appears that the DNA plays an important role in porphyrin metal complexation, which is further promoted during the HPLC step. The ability of DNA to promote the metallation of porphyrins had been previously observed by Li and Sen.³⁹

3. Conclusions

In conclusion, we have synthesized a series of water-soluble porphyrin–DNA and metalloporphyrin–DNA conjugates. Porphyrin carboxylate **1**, and Zn(II)- and Cu(II)-porphyrin derivatives have been attached to the 5' position of thymine via a non-charged amide bond applying two complementary synthetic strategies. Spontaneous metallation of porphyrin in free-base porphyrin–DNA conjugates **6** has been observed under mild conditions. We believe that trace metals in the commercial, concentrated aqueous ammonia are the origin of the unexpected metallation of the por-

phyrins. MALDI-TOF and UV-vis analysis have been employed to identify the zinc and copper in metallated species. We anticipate that the short non-charged amide linker together with different metals in the coordination center of the porphyrin will exhibit new spectroscopic and binding properties in porphyrin–DNA conjugates and help to further understand the physicochemical properties of porphyrin-capped DNA oligomers. Indeed, on-going UV, CD, and fluorescence spectroscopic studies on these porphyrin–DNA conjugates provide evidence for through space exciton coupling, intermolecular porphyrin–porphyrin stacking, and porphyrin end-capping effects of the DNA oligomers as influenced by environmental conditions. The results of these studies will be published elsewhere.

4. Experimental

Reagents and materials were obtained from commercial suppliers and used as received. Pre-dried dichloromethane (DCM) was freshly distilled from CaH₂ under argon before each use. If necessary, the reactions were performed in vacuum dried glassware under argon. Purification was performed by flash column chromatography using Machery-Nagel silica gel (0.04–0.063 mm). TLC was performed on Merck TLC plates silica gel 60 F₂₅₄ utilizing UV light (254 nm). ODNs attached to 1000 Å controlled pore glass solid-support cartridges were prepared on an ABI-380 nucleic acid synthesis system. DNA purification cartridges (Puri-Pak 0.2 μ M), activation reagent (0.45 M tetrazole/acetonitrile), and oxidation solution (0.02 M iodine/pyridine/H₂O/THF) were purchased from ChemGenes Corporation.

The porphyrin–ODNs were purified on a Waters Delta HPLC with Waters In-line Degasser AF system using a Waters reverse phase X-Terra semipreparative column MS C18 2.5 μ m 10 \times 50 mm at 50 °C, 1 mL/min flow. Evaporation of fractions from HPLC was done using a CentriVap Concentrator with a CentriVap Cold Trap.

Mass spectra were measured on a JMSHX110/110 Tandem mass spectrometer (JEOL, Tokyo, Japan) under Fast Atom Bombardment (FAB) 10 kV Accel-volt conditions with *meta*-Nitro Benzyl Alcohol (*m*-NBA) as the matrix. MALDI-TOF-MS were performed on a Voyager Applied Biosystems spectrometer using 3-HPA and diammonium citrate in 50% MeCN in H₂O. 400 MHz ¹H NMR, 75 MHz ¹³C NMR, and 162 MHz ³¹P NMR spectra were obtained on a Bruker Avance spectrometer and are reported in ppm (δ) with coupling constants in Hertz (Hz). ¹H spectra were referenced to different internal standards, TMS, DMSO, and MeOH. ³¹P spectra were referenced to an external 85% aqueous H₃PO₄ standard. UV-vis spectra were recorded on a JASCO V-530 spectrophotometer.

4.1. Synthesis of porphyrin–thymidine building blocks

4.1.1. 5'-Porphyrin-CONH-3'-hydroxythymidine (**8**)

Porphyrin carboxylate **1** (45 mg, 0.068 mmol) was dissolved under argon in dry DCM (2 mL). To the purple solution, 5'-amino-3'-hydroxythymidine (18.0 mg, 0.075 mmol), DMAP (16.6 mg, 0.136 mmol), HOBt (9.19 mg, 0.068 mmol), and EDC (26.1 mg, 0.136 mmol) were added. The solution was stirred at room temperature for 3 h. The crude reaction mixture was loaded directly onto a silica gel column and eluted using a mixture of DCM/MeOH 95:5 with 1% of triethylamine (TEA) to give 48.1 mg of **8**. Porphyrin–thymidine **8** was then dissolved in 25 mL DCM and washed with water to remove the triethylammonium salt impurity. The organic phase was dried with MgSO₄, filtered, and evaporated to dryness. 43.2 mg (72%) of **8** as a purple powder was obtained. TLC (MeOH/DCM, 1:9) *R_f* = 0.34. ¹H NMR (400 MHz, MeOH-*d*₄): 1.91 (3H, s, CH₃), 2.35 (2H, t, *J* = 5.5 Hz), 3.84 (2H, m), 4.17 (1H, m), 4.48 (1H, m), 6.26 (1H, t, *J* = 6.5 Hz), 7.60 (1H, s), 7.86 (3H, m), 8.12–8.29 (10H, m), 8.80 (8H, br s), 9.00 (4H, m). ¹³C NMR (75 MHz, MeOH-*d*₄): 13.2, 41.0, 43.8, 73.9, 87.4, 87.9, 112.6, 120.1, 120.4, 122.2, 125.5, 127.8, 132.2, 135.9, 136.5, 138.1, 139.1, 147.0, 149.8, 153.2, 161.8, 167.2, 171.0. FAB-HRMS Calcd for C₅₂H₄₁N₁₀O₅ [MH⁺] 885.3261, found 885.3249.

4.1.2. 5'-Porphyrin-CONH-thymidine-3'-phosphoramidite (**9**)

5'-Porphyrin-CONH-3'-hydroxythymidine **8** (8.5 mg, 9.61 μmol) was dissolved in 0.5 mL dry DCM under argon at room temperature. DIPEA (16.7 μL, 96.1 μmol) was added and the resulting solution was placed in an ice bath. 2-Cyanoethyl-*N,N*-diisopropylchlorophosphoramidite (10.7 μL, 48.0 μmol) was added via a syringe. The reaction mixture was stirred for 60 min at 0 °C. The crude reaction mixture was carefully loaded directly onto a silica gel column and eluted with DCM/MeOH 95:5 with 2% of TEA using an argon flow. After evaporation of the solvents, **9** was used immediately in the next reaction. The prepared amount was used for a 1 μmol ODN solid-phase synthesis (using 1 μmol scale solid support). TLC: (DCM/MeOH/TEA, 95:5:2), *R_f* = 0.35. ³¹P NMR (162 MHz, CDCl₃): 148.3, 149.3. ¹H NMR (400 MHz, CDCl₃): 1.21 (6H, 2 × CH₃), 1.24 (6H, 2 × CH₃), 1.96 (3H, s), 2.49 (2H, m), 2.69 (2H, t), 2.75 (2H, m), 3.66 (1H, m), 3.85 (2H, t, *J* = 6 Hz), 3.92 (1H, m), 4.39 (1H, m), 4.69 (1H, m), 6.07 (1/2H, t, *J* = 6.5 Hz, first diastereomer), 6.17 (1/2H, t, *J* = 6.5 Hz, second diastereomer), 7.72 (3H, m), 8.11 (4H, m), 8.24 (6H, m), 8.84 (8H, m), 9.14 (4H). FAB-HRMS Calcd for C₆₁H₅₈N₁₂O₆P [MH⁺] 1085.4262, found 1085.4336; Calcd for C₆₁H₅₈N₁₂O₇P [MH⁺] (over-oxidized side product) 1101.4211, found 1101.4336.

4.1.3. General procedure for synthesis of metallated porphyrin carboxylate Zn-1 and Cu-1

Porphyrin carboxylate **1** (0.53 mmol) and M(OAc)₂ (5.3 mmol) were mixed in chloroform (90 mL) under argon atmosphere and refluxed for 5.5 h. The reaction mixture was allowed to cool to room temperature, washed with an aqueous solution of EDTA (10 equiv, 200 mL) to remove excess M(II) acetate, then three times with brine, dried over Na₂SO₄, and concentrated. The product was characterized by UV–vis absorption, FAB mass spectrometry, and ¹H NMR spectroscopy. Metalloporphyrins **M-1** were pure according to ¹H NMR and FAB MS and were used in the next reaction without further purification.

4.1.3.1. Zinc porphyrin carboxylate Zn-1. FAB-HRMS Calcd for C₄₂H₂₆N₇O₂Zn (MH⁺) 724.1369, found 724.1464. UV–vis in MeOH: 417 nm (ε = 334,300), 554 nm (ε = 12,200), 592 nm (ε = 3200).

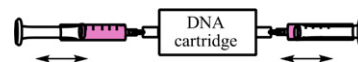
4.1.3.2. Copper porphyrin carboxylate Cu-1. FAB-HRMS Calcd for C₄₂H₂₆N₇O₂Cu (MH⁺) 723.1544, found 723.1444. UV–vis in CH₂Cl₂:

414 nm (ε = 137,000), 533 nm (ε = 8600) The UV–vis absorption bands for the copper porphyrin **Cu-1** are very broad because of partial aggregation.

4.2. Porphyrin–oligodeoxynucleotide solid-phase synthesis and purification

4.2.1. Approach 1

Using an ABI-380 DNA synthesizer, unmodified ODNs 5'-hydroxy-(GC)_{*n*}GCA-support **3a–c** (*n* = 1–3) were prepared using a 1000 Å CPG solid-support cartridge. The 5'-monomethoxytrityl (MMT)-protected 5'-amino-5'-deoxy-thymidine-phosphoramidite was coupled to the solid supported ODNs **3a–c** under standard phosphorylation conditions, and the MMT protecting group was removed with trichloroacetic acid to give solid supported 5'-amino modified ODNs **4a–c**. Conjugation of the exposed 5'-amino-group of thymidine in ODNs **4a–c** with porphyrin carboxylic acid **1** was then carried out manually on a column cartridge under the following conditions: porphyrin carboxylic acid **1** (28 mg, 0.038 mmol) was added to a mixture of PyBOP (benzotriazol-1-yl-oxy-tris-pyrrolidino-phosphonium hexafluorophosphate, 21 mg, 0.04 mmol) and DIPEA (13 μL, 0.071 mmol) dissolved in dry DMF (0.5 mL). This reaction mixture was injected into a pre-washed (0.5 mL DMF plus 13 μL DIPEA) column cartridge (CPG 1000 Å) containing the 5'-amino-terminal oligonucleotides **4a–c** attached to the solid support. Two syringes were connected to the DNA cartridge as shown below, one empty and the other with DMF plus the DIPEA solution. The reaction mixture was then slowly passed through the column into the other syringe in a back-and-forth manner every 15 min for 2 h at room temperature in the dark. The column cartridge saturated with the reaction mixture was then allowed to sit in the column for additional 10 h at room temperature.



The column was next washed with DMF (1 mL) to remove the reaction mixture until the eluent was clear, and then three further times with 1 mL aliquots of DMF. The washes were pushed back and forth through the column to optimize removal of unreacted porphyrin. The column was then regenerated with eight 1 mL washes of acetonitrile (MeCN), followed by drying the column with a flow of nitrogen gas.

4.2.2. Cleavage from resin and deprotection

In order to cleave the porphyrin–ODN from the cartridge, 800 μL of high grade, concentrated aqueous ammonia (Aldrich, 28% in water, 99.99+%) was injected into the column containing the prepared porphyrin–ODN conjugate, and the ammonia solution pushed back and forth using the two-syringe procedure, again in the dark. Care must be taken to ensure that no air bubbles are introduced. After the cleavage reaction mixture was allowed to stand for 12 h at room temperature, the colored solution was slowly pushed through the column cartridge back and forth every 15 min for an additional hour (a total of 4 back-and-forth exchanges). The ammonia solution was collected and concentrated under vacuum and then freeze-dried to provide crude porphyrin–DNA conjugates **6a**, **6b**, or **6c**, respectively. MALDI-TOF mass spectrum analysis indicated the presence of mostly the desired porphyrin–DNA conjugates **6**.

4.2.3. Approach 2

Porphyrin–ODNs were synthesized on 1 μmol scale CPG solid support (pore size on 1000 Å) using an 'in flask' synthesis.³⁷ The freshly synthesized 5'-porphyrinthymidine 3'-phosphoramidite **9**

(9.60 μmol) was dissolved in activating reagent (0.5 mL, 0.45 M tetrazole/acetonitrile) under dry argon at room temperature. The commercially available solid supported DNA **10a–c** was added to this solution in one portion against a positive pressure of argon. The reaction mixture was stirred without using a stir bar for 45 min at room temperature. After filtration and washing of the beads with acetonitrile, and DCM, oxidation reagent was added (1 mL, 0.02 M, iodine in $\text{H}_2\text{O}/\text{THF}/\text{pyridine}$) for 5 min. The solution was then filtered and the solid-support washed repeatedly with MeCN and MeOH, followed by a single wash with DCM to reveal a red-colored resin.

4.2.4. Cleavage from resin and deprotection

Eight hundred microliters of high grade, concentrated ammonia solution (28% ammonia hydroxide) was added to the 1 μmol resin containing the prepared porphyrin–DNA conjugates **5a–c** in a screw cap vial. After an incubation period of 2 h with moderate shaking, the red supernatant containing the cleaved porphyrin–ODN was transferred (without the resin) to a screw cap vial. The complete deprotection was achieved in 24 h at room temperature with occasional shaking.

The crude porphyrin–ODN was then purified using a DNA Puri-Pak oligonucleotide purification cartridge (OPC) from ChemGenes. The Puri-Pak purification cartridge was first pre-washed with MeCN (5 mL) and high purity water (20 mL). Water (1.5 mL) was added to the pink-red ammonia solution containing the porphyrin–DNA conjugate **6a** and the mixture slowly injected into the OPC, again using the two-syringe technique. The column was washed with 20 mL of water, and this was repeated three times until the eluate was colorless. The column usually retained a slight pink color. A final wash with MeCN/ H_2O solution was combined with the previous fractions and concentrated under reduced pressure to half its initial volume. Finally, the concentrated solution was transferred into a 1.5 mL plastic tube and lyophilized using a CentriVap Concentrator and cold trap. The same procedure was used for porphyrin–DNA conjugates **6b** and **6c**.

4.2.5. Cartridge purification of porphyrin–DNA conjugates **6a**, **6b**, and **6c**

The crude porphyrin–DNA was pre-purified using DNA Puri-Pak purification cartridges from ChemGenes. The Puri-Pak purification cartridge was pre-equilibrated by washing two times with 2.5 mL acetonitrile followed by three times with 3 mL of 1.0 M triethylammonium acetate (TEAA). High purity water (800 μL) was added to the 1 μmol resin in 800 μL highly graded, concentrated ammonia solution. The diluted ammonia solution (1600 μL) was then loaded onto the pre-equilibrated cartridge. The cartridge was first washed with 3% NH_4OH followed by high purity water in order to remove any failure sequences. The desired porphyrin–DNA conjugates **6** were then eluted using a 1:1 mixture of water/acetonitrile. The collected red solution containing conjugates **6** was concentrated under reduced pressure, and dried under high vacuum. The porphyrin–ODN conjugates **6a** (porphyrin-hexamer), **6b** (porphyrin-octamer), and **6c** (porphyrin-decamer) were then stored at -20°C under argon.

4.2.6. HPLC purification of porphyrin–DNA conjugates **6a–c**

The purification of the crude mixture of porphyrin–ODN conjugates **6a–c** was achieved on a Waters Delta HPLC with a Waters In-line Degasser AF system and a Water's reverse phase X-Terra semi-preparative column MS C18 2.5 μm 10 \times 50 mm at 50°C . A gradient of methanol and buffer (38.1 mM hexafluoroisopropanol and 8.4 mM triethylamine in water) and 1 mL/min flow was used (Table 3).³⁷ The pre-purified porphyrin–DNA conjugate (the amount originating from 1 μM oligonucleotide synthesis) was dissolved in a minimal amount of water and injected onto the HPLC. The

Table 3

HPLC condition for purification of porphyrin–DNA conjugates **2H-6b**, **Zn-6b**, and **Cu-6b**

Time (min)	Buffer ^a (%)	MeOH (%)
0	88	12
60	40	60
63	10	90
90	10	90

^a Buffer: 38.1 mM hexafluoroisopropanol (HFIP) + 8.4 mM TEA in water.

diode array detector (DAD) showed two absorption maxima for two major peaks, one at ~ 420 nm and another at ~ 260 nm. The peaks were collected in 1.5 mL plastic tubes and evaporated using CentriVap Concentrator with a CentriVap Cold Trap. Table 3 summarizes retention times of all porphyrin–DNA conjugates **6a–c**.

The dried, purified porphyrin–ODN conjugate **6b** was dissolved in water, and the yield of porphyrin–ODN conjugate determined by UV–vis spectroscopy using an extinction coefficient at 260 nm of $72,300\text{ M}^{-1}\text{ cm}^{-1}$ for the single-stranded TGCGCGCA oligomer. The HPLC recovery yields are calculated based on the intensities of the product peak from the crude HPLC traces recorded at 50°C as reported previously.¹⁶ Porphyrin–DNA conjugate **Zn-6b**: yield = 35%, porphyrin–DNA conjugate **Cu-6c**: yield = 32% (both intentionally prepared from metalloporphyrins **Zn-1** and **Cu-1**).

Acknowledgments

The authors gratefully acknowledge financial support from the following agencies: NSF (REU) grant to A.W.; Columbia University FOSTOR grant to S.C.; and the University of Catania, Italy for a scholarship to A.M. We also wish to thank Regina Monaco for helpful discussions.

Supplementary data

Supplementary data associated with this article can be found, in the online version, at doi:10.1016/j.bmc.2008.05.041.

References and notes

- Nakamura, Y.; Aratani, N.; Osuka, A. *Chem. Soc. Rev.* **2007**, 36, 831.
- Hoeben, F. J. M.; Wolffs, M.; Zhang, J.; De Feyter, S.; Leclerc, P.; Schenning, A.; Meijer, E. W. *J. Am. Chem. Soc.* **2007**, 129, 9819.
- Imahori, H. *J. Phys. Chem. B* **2004**, 108, 6130.
- Lin, V. S.; DiMaggio, S. G.; Therien, M. J. *Science* **1994**, 264, 1105.
- Kuimova, M. K.; Hoffmann, M.; Winters, M. U.; Eng, M.; Balaz, M.; Clark, I. P.; Collins, H. A.; Tavender, S. M.; Wilson, C. J.; Albinsson, B.; Anderson, H. L.; Parker, A. W.; Phillips, D. *Photochem. Photobiol. Sci.* **2007**, 6, 675.
- Anderson, H. L. *Chem. Commun.* **1999**, 2323.
- Mayer-Enthart, E.; Wagenknecht, H. A. *Angew. Chem. Int. Ed.* **2006**, 45, 3372.
- Fendt, L. A.; Bouamaied, I.; Thoni, S.; Amiot, N.; Stulz, E. J. *Am. Chem. Soc.* **2007**, 129, 15319.
- Endo, M.; Shiroyama, T.; Fujitsuka, M.; Majima, T. *J. Org. Chem.* **2005**, 70, 7468.
- Guckian, K. M.; Schweitzer, B. A.; Ren, R. X.-F.; Scheils, C. J.; Paris, P. L.; Tahmassebi, D. C.; Kool, E. T. *J. Am. Chem. Soc.* **1996**, 118, 8182.
- Martray, T. J.; Kool, E. T. *J. Am. Chem. Soc.* **1998**, 120, 6191.
- Narayanan, S.; Gall, J.; Richert, C. *Nucleic Acids Res.* **2004**, 32, 2901.
- Tuma, J.; Paulini, R.; Rojas Stutz, J. A.; Richert, C. *Biochemistry* **2004**, 43, 15680.
- Kryatova, O. P.; Connors, W. H.; Blecinski, C. F.; Mokhir, A. A.; Richert, C. *Org. Lett.* **2001**, 3, 987.
- Dogan, Z.; Paulini, R.; Rojas Stutz, J. A.; Narayanan, S.; Richert, C. *J. Am. Chem. Soc.* **2004**, 126, 4762.
- Tuma, J.; Connors, W. H.; Stitelman, D. H.; Richert, C. *J. Am. Chem. Soc.* **2002**, 124, 4236.
- Balaz, M.; Li, B. C.; Ellestad, G. A.; Berova, N. *Angew. Chem. Int. Ed.* **2006**, 45, 3530.
- Shaw, J.-P.; Kent, K.; Bird, J.; Fishback, J.; Froehler, B. *Nucleic Acids Res.* **1991**, 19, 747.
- Fiel, R. J. *J. Biomol. Struct. Dyn.* **1989**, 6, 1259.
- Pasternack, R. F. *Chirality* **2003**, 15, 329.
- Pasternack, R. F.; Gibbs, E. J. *ACS Symp. Ser.* **1989**, 402, 59.
- Marzilli, L. G. *New J. Chem.* **1990**, 14, 409.

23. Balaz, M.; De Napoli, M.; Holmes, A. E.; Mammana, A.; Nakanishi, K.; Berova, N.; Purrello, R. *Angew. Chem. Int. Ed.* **2005**, *44*, 4006.
24. Pitié, M.; Casas, C.; Lacey, C. J.; Pratviel, G.; Bernadou, J.; Meunier, B. *Angew. Chem., Int. Ed. Engl.* **1993**, *32*, 557.
25. Bigey, P.; Pratviel, G.; Meunier, B. *Nucleic Acids Res.* **1995**, *23*, 3894.
26. Balaz, M.; Bitsch-Jensen, K.; Mammana, A.; Ellestad, G. A.; Nakanishi, K.; Berova, N. *Pure Appl. Chem.* **2007**, *79*, 801.
27. Murashima, T.; Hayata, K.; Saiki, Y.; Matsui, J.; Miyoshi, D.; Yamada, T.; Miyazawa, T.; Sugimoto, N. *Tetrahedron Lett.* **2007**, *48*, 8514.
28. Sitaula, S.; Reed, S. M. *Bioorg. Med. Chem. Lett.* **2008**, *18*, 850.
29. Balaz, M.; Holmes, A. E.; Benedetti, M.; Rodriguez, P. C.; Berova, N.; Nakanishi, K.; Proni, G. *J. Am. Chem. Soc.* **2005**, *127*, 4172.
30. Endo, M.; Fujitsuka, M.; Majima, T. *Tetrahedron* **2008**, *64*, 1839.
31. Endo, M.; Fujitsuka, M.; Majima, T. *J. Org. Chem.* **2008**, *73*, 1106.
32. Balaz, M.; Steinkruger, J. D.; Ellestad, G. A.; Berova, N. *Org. Lett.* **2005**, *7*, 5613.
33. Berlin, K.; Jain, R. K.; Simon, M. D.; Richert, C. J. *Org. Chem.* **1998**, *63*, 1527.
34. Balaz, M.; Li, B. C.; Steinkruger, J. D.; Ellestad, G. A.; Nakanishi, K.; Berova, N. *Org. Biomol. Chem.* **2006**, *4*, 1865.
35. Mag, M.; Engels, J. W. *Nucleic Acids Res.* **1989**, *17*, 5973.
36. Hu, X.; Tierney, M. T.; Grinstaff, M. W. *Bioconjugate Chem.* **2002**, *13*, 83.
37. Balaz, M.; Holmes, A. E.; Benedetti, M.; Proni, G.; Berova, N. *Bioorg. Med. Chem.* **2005**, *13*, 2413.
38. Dorough, G. D.; Miller, J. R.; Huennekens, F. M. *J. Am. Chem. Soc.* **1951**, *73*, 4315.
39. Li, Y. F.; Sen, D. *Nat. Struct. Biol.* **1996**, *3*, 743.